Bifurcation in Dynamical Systems. Deterministic Chaos. Quantum Chaos

Izvestiya Vysshikh Uchebnykh Zavedeniy. Applied Nonlinear Dynamics. 2025;33(6)

Article DOI: 10.18500/0869-6632-003172

On the interaction of a system with multifrequency oscillations with a chaotic generator

A. P. Kuznetsov[1], *L. V. Turukina*[1,2] ✉

[1]Saratov Branch of Kotelnikov Institute of Radioengineering and Electronics, Russia
[2]Saratov State University, Russia
E-mail: kuzalexp@yandex.ru, ✉turukinalv@yandex.ru

Received 17.01.2025, accepted 2.04.2025, available online 22.04.2025, published 28.11.2025

Abstract. The *purpose* of the work is to study the influence of the dynamics of a chaotic system on a system with multi-frequency quasi-periodicity and the Landau–Hopf scenario. The Kislov–Dmitriev chaotic system and an ensemble of van der Pol oscillators with non-identical excitation parameters are chosen as the object of study. *Methods.* The analysis was carried out using graphs of Lyapunov exponents and the criterion for identifying types of quasiperiodic bifurcations based on them. *Results.* Scenarios of the changing of the regime's types are presented as the coupling parameter between the subsystems decreased. They may have certain features. Thus, the transition from a three-frequency to a four-frequency regime occurs not through a quasiperiodic Hopf bifurcation, but through a chaos window. The latter is characterized by three or four zero Lyapunov exponents. Inside this chaotic window, a peculiar bifurcation is possible. It is corresponding to an increase in the number of zero Lyapunov exponents according to the type of a saddle-node Hopf bifurcation. Chaos with a different number of zero exponents is observed as the coupling parameter of van der Pol oscillators varied. In this case, a cascade of points corresponding to a step-by-step increase in the number of zero exponents occurs according to a different scenario. It is to a certain extent similar to a quasiperiodic Hopf bifurcation. When the control parameter When the control parameter of the Kislov–Dmitriev system increases, hyperchaos with three zero Lyapunov exponents may appear in the combined system. An inverted order of changing modes is also possible. In this case, for example, a three-frequency regime turns into a four-frequency regime through a chaotic window. *Conclusion.* The obtained results expand conception about high-dimensional chaos with several zero Lyapunov exponents and its transformations with parameter changes.

Keywords: chaos, hyperchaos, quasi-periodicity, Lyapunov exponents, bifurcations.

Acknowledgements. The work was carried out within the framework of the state assignment of the V. A. Kotelnikov IRE RAS (FFWZ-2025-0016), Russia.

For citation: Kuznetsov AP, Turukina LV. On the interaction of a system with multifrequency oscillations with a chaotic generator. Izvestiya VUZ. Applied Nonlinear Dynamics. 2025;33(6):785–803. DOI: 10.18500/0869-6632-003172

Introduction

The study of coupled oscillators is one of the important tasks of nonlinear oscillation theory in general and its applications, for example, in radiophysics and electronics [1–4]. The development of computer technology and the theory of dynamical systems and its applications in relation to multidimensional systems [5–10] makes the problem of oscillations relevant not only in the classical case of two subsystems, but also in a larger number of [11–14]. In this case, individual subsystems may exhibit any of the main types of vibrations. These can be autonomous periodic, quasi-periodic, or chaotic modes. The issue of the interaction of subsystems with different types of vibrations is poorly studied. In this regard, we will pay attention to the case when multi-frequency quasi-periodic oscillations are possible in the first subsystem, and chaos in the second.

It can be noted here that the relationship between quasi-periodic and chaotic dynamics has attracted attention since the famous works of Landau and Hopf [15,16]. In the scenario that received their name, the oscillations gradually become more complex due to the addition of new frequency components to the spectrum as a result of a cascade of quasi-periodic Hopf bifurcations. Despite the criticism of Ruel and Takens [17], reports on the possibility of stable multi-frequency oscillations (which invariant tori of high dimension correspond to in phase space) periodically appear in the literature [18–28]. The same applies to a certain extent to the Landau-Hopf scenario [29–37]. This raises the question of the interaction of systems with invariant tori and chaos. In [38,39], the simplest version of this situation was considered. A generator capable of demonstrating autonomous two-frequency quasi-periodic dynamics associated with a chaotic Ressler system was studied. In [40], an ensemble of five van der Pol oscillators [34] was used as the first subsystem in a similar formulation of the problem. This system is capable of demonstrating quasi-periodic oscillations with a different number of incommensurable frequencies. As the coupling of the oscillators decreases, a cascade of bifurcations is observed for it, corresponding to several steps of the Landau-Hopf scenario. Here we will discuss the case of the connection of the [34] subsystem with the chaotic Kislov-Dmitriev system. The latter can act as one of the basic chaotic systems [41–44]. We will pursue a twofold goal. First, to find out to what extent the results of [40] are universal. Secondly, it is necessary to demonstrate new points in relation to [40], which are related, in particular, to the possible modification of the attractor in a chaotic subsystem with an increase in the nonlinearity parameter. We also note that the formulated problem turns out to be related to the problem of chaos with additional zero Lyapunov exponents, see the corresponding references further in the section 4.

1. Quasi-periodic subsystem

Our chosen quasi-periodic subsystem [34] is an ensemble of five globally connected van der Pol oscillators:

$$\ddot{x_n} - (\lambda_n - x_n^2)\dot{x_n} + \left(1 + \frac{n-1}{4}\Delta\right) x_n + \frac{\mu}{4}\sum_{i=1}^{5}(\dot{x_n} - \dot{x_i}) = 0. \tag{1}$$

Here λ_n is the excitation parameter of the nth oscillator, n varies from 1 to 5, Δ determines the frequency disorder of the oscillators, and the frequency of the first one is taken as one, μ is the dissipative coupling parameter.

This system has the following features that enable multiple steps of the Landau-Hopf scenario. The oscillators are not identical in terms of excitation parameters λ_n, which ensures a step-by-step output of the corresponding modes beyond the excitation threshold with a decrease in the coupling value (analogous to the Reynolds number). Due to the Δ factor, all oscillators are upset in their natural frequency, and we will choose a large disorder, which eliminates the effects of synchronization. The ensemble is organized according to the principle of a network, where everyone is connected to everyone. In this case, the excitation parameter of each individual oscillator λ_n controls the corresponding quasi-periodic bifurcation of the entire ensemble.

Here and further, following [34,40], we set the excitation parameters $\lambda_1 = 0.1$, $\lambda_2 = 0.2$, $\lambda_3 = 0.3$, $\lambda_4 = 0.4$, $\lambda_5 = 0.5$. In this case, due to the non-identity of the parameters λ_n, the fifth oscillator is characterized by the largest, and the first one by the smallest value of the excitation parameter. The value of the frequency offset is set to $\Delta = 3$. Then, with a decrease of μ at $\mu \approx \lambda_n$, the Andronov-Hopf

bifurcation of the limit cycle from equilibrium, the Neumark-Sacker bifurcation of the birth of a two-frequency torus, and then three quasi-periodic bifurcations of the soft occurrence of three-, four- and five-frequency tori.

2. Chaotic subsystem

As a chaotic subsystem, we use the Kislov-Dmitriev system [41–44]. Physically, it is a generator in the form of a ring-enclosed chain of a nonlinear amplifier, an RLC filter, and an inertial element. Such a system is described by the equations:

$$\begin{aligned} &\ddot{x} + \frac{1}{Q}\dot{x} + \omega_0^2 x = z, \\ &T\dot{z} + z = Mx\exp(-x^2). \end{aligned} \tag{2}$$

The convenience of the system (2) for further investigation is that the first equation is a traditional oscillator relative to the variable x, excited by the variable z. In this context, Q is the attenuation parameter (Q-factor), and ω_0 is the natural frequency of this oscillator. Also in (2) M — this is the main parameter of nonlinearity responsible for the occurrence of chaos.

Note that in the equations (2), the natural frequency ω_0 can be eliminated by renormalizing the parameters $Q \to Q/\omega_0$, $T \to T/\omega_0$, $M \to M\omega_0^2$ and variables $t \to t/\omega_0$, $z \to z\omega_0^2$. Then the system (2) is reduced to the canonical form [43] with $\omega_0 = 1$. However, since the frequency of the first van de Pol oscillator is assumed to be one in the quasi-periodic subsystem (refeq1), we will use equations in the form (refeq2) to ensure the frequency decoupling of all oscillators. Next, we set $\omega_0 = 0.5$, so that this frequency does not coincide with any of the natural frequencies of the van der Pol oscillators (1).

The choice of the main control parameter M also requires explanation. In Fig. 1 shows graphs of Lyapunov exponents Λ_i of an individual system (2) depending on the value of M for $T = 10$ and $Q = 20$.

It can be seen that a cascade of doubling bifurcations of periodic modes of PD occurs in the system, the sign of which is the conversion to zero of the second indicator Λ_2 at the bifurcation points. As a result, a chaotic attractor appears according to the Feigenbaum scenario [43], the phase portrait of which is shown in Fig. 2, *a*. For convenience of perception, the corresponding value of the parameter M is marked with an arrow in Fig. 1. Next, there is a wide window of periodic modes, and then — chaos again. The corresponding attractor is shown in Fig. 2, *b*. It can be seen that his device differs from Fig.

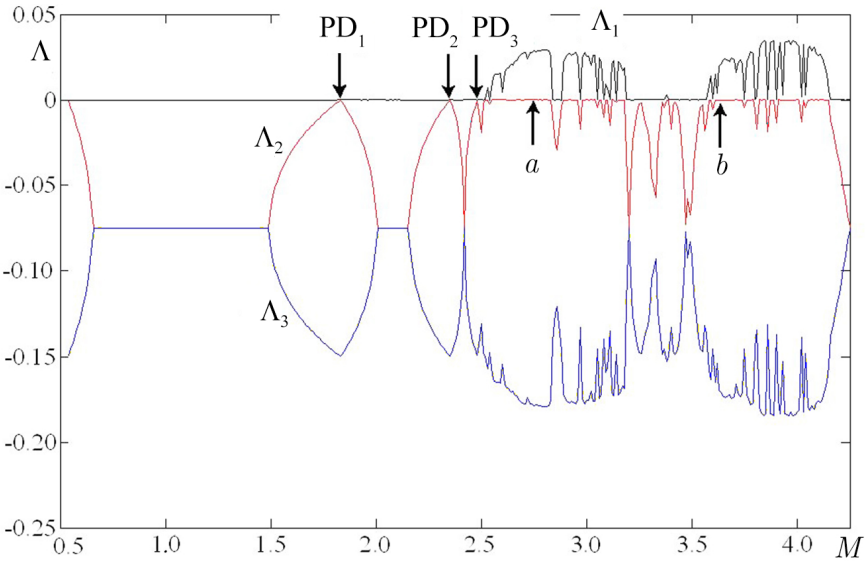

Fig. 1. Graphs of the Lyapunov exponents of the Kislov–Dmitriev system (2) on the parameter M. $T = 10$, $Q = 20$, $\omega_0 = 0.5$. The arrows with the letters (a) and (b) indicate the points corresponding to Fig. 2 (color online)

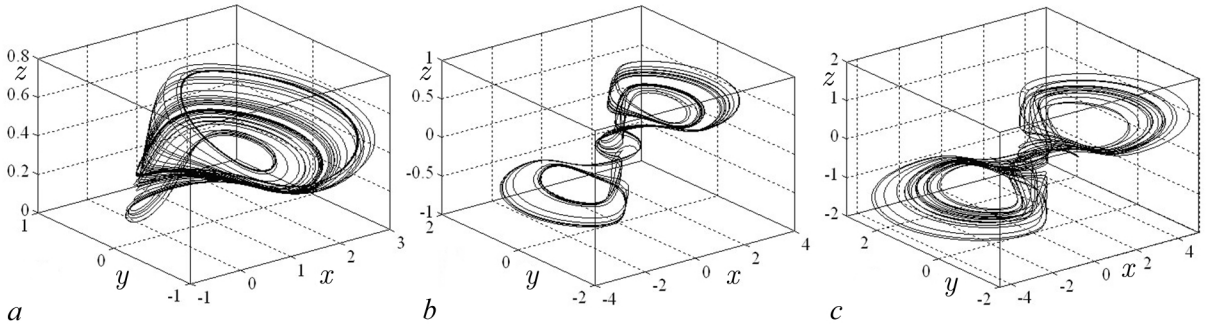

Fig. 2. Phase portraits of the chaotic attractor of the Kislov–Dmitriev system (2) for $M = 2.75$ (a), $M = 3.65$ (b) and $M = 8.2$ (c); $T = 10$, $Q = 20$, $\omega_0 = 0.5$

2, a, although the senior Lyapunov exponents are close in both cases (respectively, $\Lambda_1 = 0.02842$ and $\Lambda_1 = 0.02354$). We will continue to use both options, the first in order to consider the case corresponding to the Feigenbaum scenario, and the second in order to study the effect of a change in the configuration of the attractor.

We will also consider the case when the parameter $M = 8.2$. The attractor in this case is shown in Fig. 2, c and is somewhat visually close to the case of Fig. 2, b. However, it is answered by a noticeably large value of the senior Lyapunov exponent — $\Lambda_1 = 0.06225$. As we will see, this leads to new dynamic features.

3. Related systems

Now we will organize the connection of the ensemble of van der Pol oscillators (1) with the chaotic Kislov-Dmitriev system (2). For convenience, the equations for each oscillator are written explicitly:

$$
\begin{aligned}
&\ddot{x_1} - (\lambda_1 - x_1^2)\dot{x_1} + x_1 + \frac{\mu}{4}(4\dot{x_1} - \dot{x_2} - \dot{x_3} - \dot{x_4} - \dot{x_5}) = 0,\\
&\ddot{x_2} - (\lambda_2 - x_2^2)\dot{x_2} + \left(1 + \frac{\Delta}{4}\right) x_2 + \frac{\mu}{4}(4\dot{x_2} - \dot{x_1} - \dot{x_3} - \dot{x_4} - \dot{x_5}) = 0,\\
&\ddot{x_3} - (\lambda_3 - x_3^2)\dot{x_3} + \left(1 + \frac{\Delta}{2}\right) x_3 + \frac{\mu}{4}(4\dot{x_3} - \dot{x_1} - \dot{x_2} - \dot{x_4} - \dot{x_5}) = 0,\\
&\ddot{x_4} - (\lambda_4 - x_4^2)\dot{x_4} + \left(1 + \frac{3\Delta}{4}\right) x_4 + \frac{\mu}{4}(4\dot{x_4} - \dot{x_1} - \dot{x_2} - \dot{x_3} - \dot{x_5}) = 0,\\
&\ddot{x_5} - (\lambda_5 - x_5^2)\dot{x_5} + (1 + \Delta)\, x_5 + \frac{\mu}{4}(4\dot{x_5} - \dot{x_1} - \dot{x_2} - \dot{x_3} - \dot{x_4}) + k(\dot{x_5} - \dot{x}) = 0,\\
&\ddot{x} + \frac{1}{Q}\dot{x} + \omega_0^2 x + k(\dot{x} - \dot{x_5}) = z,\\
&T\dot{z} + z = Mx\exp(-x^2).
\end{aligned}
\tag{3}
$$

Here, for certainty, communication is carried out through the fifth van der Pol oscillator and is controlled by the k parameter. As we noted, the first equation of the Kislov-Dmitriev system has the form of an oscillator relative to the variable x. The connection in (3) is arranged taking this analogy into account through the member $\pm k(\dot{x_5} - \dot{x})$. The addition of variables through the rates of change, as in the case of the simplest oscillators, provides the dissipative nature of the connection that is necessary for us and the ability to compare with the results of [40]. Note that such a connection of the Kislov-Dmitriev system with a single van der Pol oscillator was used in [45], which led to some interesting features of the dynamics. We will not touch here on the circuit implementation of the system (3), it can be considered as an independent dynamic system of high dimension.

4. Transformations of attractors with additional zero Lyapunov exponents and bifurcation of invariant tori

Consider the system (3). First, we select the values of the parameters $\mu = 0.25$ and $\Delta = 3$, which, according to [34], corresponds to the three-frequency mode in the quasi-periodic subsystem. In Fig. 3 graphs of the dependence of eight Lyapunov exponents are shown[1] of the combined system (3) from the connection parameter k. They can be used to identify the type of observed mode according to the Table. The Table contains seven Lyapunov exponents, the rest are always negative.

In the right part of Fig. 3 you can see the three-frequency mode $3T$ (3-torus) with $\Lambda_{1,2,3} = 0$. Thus, the interaction of chaotic and quasi-periodic subsystems led to the suppression of chaos. In this case, the number of incommensurable frequencies corresponds to the oscillation mode in the quasi-periodic subsystem.

With a decrease in communication, a transition to the four-frequency mode of $4T$ is observed. Thus, the dimension of the quasi-periodic mode increases by one, with the additional frequency introduced by the chaotic subsystem. The same effect is typical for the case of a chaotic subsystem in the form of a Ressler system [40]. However, for her, this transition is happening

exclusively through one classical quasi-periodic Hopf bifurcation. In this case, the scenario is more complicated. When the coupling decreases, we first enter the resonant window of the two-frequency mode with $\Lambda_{1,2} = 0$. It is bounded on both sides by lines of saddle-node bifurcations of two-frequency tori $QSN_{1,2}$. The type of bifurcation is determined by the behavior of Lyapunov exponents in accordance with the criterion [46]. The resonant window and bifurcations of this type correspond to the characteristic «failure» of the third indicator Λ_3 in the negative region.

After exiting this window, a three-frequency torus with $\Lambda_{1,2,3} = 0$ is again observed to the left of it in the narrow region of the parameter, provided $\Lambda_4 < 0$. However, almost immediately there is chaos C. At the corresponding point Q_1, the exponent Λ_4 turns to zero, and the exponent Λ_1 becomes positive. The result is chaos, but with a special feature - the presence of not one, but three zero Lyapunov exponents $\Lambda_{2,3,4} = 0$.

Reduce the connection parameter k. As we approach the point Q_2, the indicator Λ_5 increases. Immediately at this point, it turns to zero and then remains zero, so now $\Lambda_{2,3,4,5} = 0$. Thus, a kind of

[1]To calculate the Lyapunov exponents, the standard Runge-Kutta method of the 4th order was used for numerical solution of differential equations, as well as the Gram-Schmidt orthogonalization method. The integration step in numerical calculations was chosen to be 0.01; the initial conditions for all dynamic variables are 0.1; the time of the transition process was on the order of 10^4 units of normalized time; the calculation time of the indicators themselves was on the order of 10^5 units of normalized time, which makes it possible to calculate Lyapunov exponents with an accuracy of $\pm 10^{-5}$.

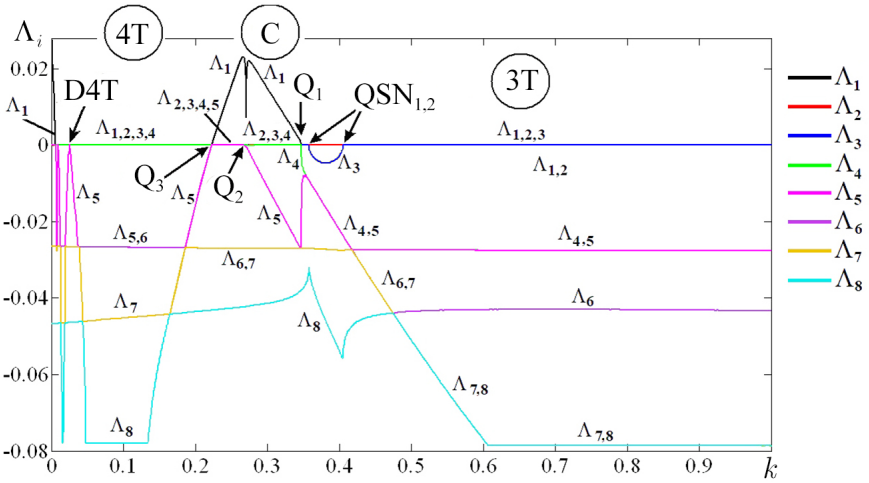

Fig. 3. Graphs of the eight Lyapunov exponents of the model (3) on the coupling parameter k; $\mu = 0.25$, $\Delta = 3$. Parameters of the Kislov–Dmitriev model are $M = 2.75$, $T = 10$, $Q = 20$, $\omega_0 = 0.5$ (color online)

Table. Types of regimes and the spectrum of Lyapunov exponents

Обозначение	Mode type	The spectrum of senior Lyapunov exponents
P	periodic (limit cycle)	$\Lambda_1 = 0,\ \Lambda_{2,3,4,5,6,7} < 0$
2T	two-frequency quasi-periodic (two-dimensional torus)	$\Lambda_{1,2} = 0,\ \Lambda_{3,4,5,6,7} < 0$
3T	three-frequency quasi-periodic (three-dimensional torus)	$\Lambda_{1,2,3} = 0,\ \Lambda_{4,5,6,7} < 0$
4T	four-frequency quasi-periodic (four-dimensional torus)	$\Lambda_{1,2,3,4} = 0,\ \Lambda_{5,6,7} < 0$
5T	five-frequency quasi-periodic (a five-dimensional torus)	$\Lambda_{1,2,3,4,5} = 0,\ \Lambda_{6,7} < 0$
6T	six-frequency quasi-periodic (six-dimensional torus)	$\Lambda_{1,2,3,4,5,6} = 0,\ \Lambda_7 < 0$
C	chaos	$\Lambda_1 > 0,\ \Lambda_{2,3,4,5,6,7} \leqslant 0$
H	hyperhaos	$\Lambda_{1,2} > 0,\ \Lambda_{3,4,5,6,7} \leqslant 0$

bifurcation of the chaotic attractor occurs, consisting in an increase in the number of zero exponents from three to four.

Finally, at the point Q_3, the chaos disappears again, and at the same time the indicator Λ_5 goes back into the negative area. The result is a four-frequency torus with $\Lambda_{1,2,3,4} = 0$. Thus, due to the nontrivial bifurcation Q_2, a three-frequency torus is observed to the right of the chaotic window, and a four-frequency torus is observed to the left.

With a further decrease in coupling, bifurcations of doubling of the four-frequency torus $D4T$ occur. One of them is clearly visible in Fig. 3. And then, with very little connection, chaos is born again. In this case, the behavior is similar to the case of [40].

As we noted, in addition to one «mandatory» in continuous-time systems, the zero value is $\Lambda_2 = 0$ two or even three more are added. The concept of a chaotic attractor with an additional zero Lyapunov exponent was presented in citeb47,b48,b49, where it was called the quasi-periodic Hainaut-like attractor. To date, examples have been found for the Lorenz-84 climate model with periodic (seasonal) exposure to [47,48], the [49] model display, the discrete version of the Lorenz-84 [50] system, coupled radiophysical generators [51], and a system of phase oscillators with biharmonic coupling [52]. More recently, an example of hyperchaosis (that is, a mode with two positive indicators) with an additional zero index [53] has also been found. In this paper, a system of three interacting encapsulated gas bubbles in a liquid was considered. The mechanisms of chaos and hyperchaosis with an additional zero Lyapunov exponent are discussed. Current examples and their discussion for mappings can also be found in [54,55]. These results relate to the case of one additional zero indicator. The case of two or more additional zero exponents was also recently presented in [38–40]. Thus, the replenishment of «collection» systems with similar dynamics is interesting and signals the typicality of this phenomenon. We also note that the topic related to the doubling of tori continues to be relevant, for example, [56,57].

Let us now illustrate the picture of modes depending on the «internal» coupling parameter of the quasi-periodic subsystem μ for two values of k, Fig. 4. In the case of a small $k = 0.0025$ in Fig. 4, *a* with a large connection μ, classical chaos is observed when $\Lambda_1 > 0$, $\Lambda_2 = 0$, and the other indicators are negative. At point L_1, the type of chaotic regime changes — now there is an additional zero Lyapunov exponent, so that $\Lambda_1 > 0$, $\Lambda_{2,3} = 0$, and the remaining indicators are negative. Then at the points L_2, L_3, L_4 and L_5 chaos ensues with two, three, four, and five additional zero Lyapunov exponents. These are some characteristic new points, we have designated them L — from Lyapunov exponents.

Note that when approaching points of this type, the negative indicators match in pairs. So, when approaching from the right to L_1, the indicators $\Lambda_3 = \Lambda_4$, when approaching L_2 — $\Lambda_4 = \Lambda_5$, etc. In this respect, the behavior is similar to the case of the quasi-periodic Hopf bifurcation [46].

Thus, we note two types of points responsible for an increase in the number of zero Lyapunov

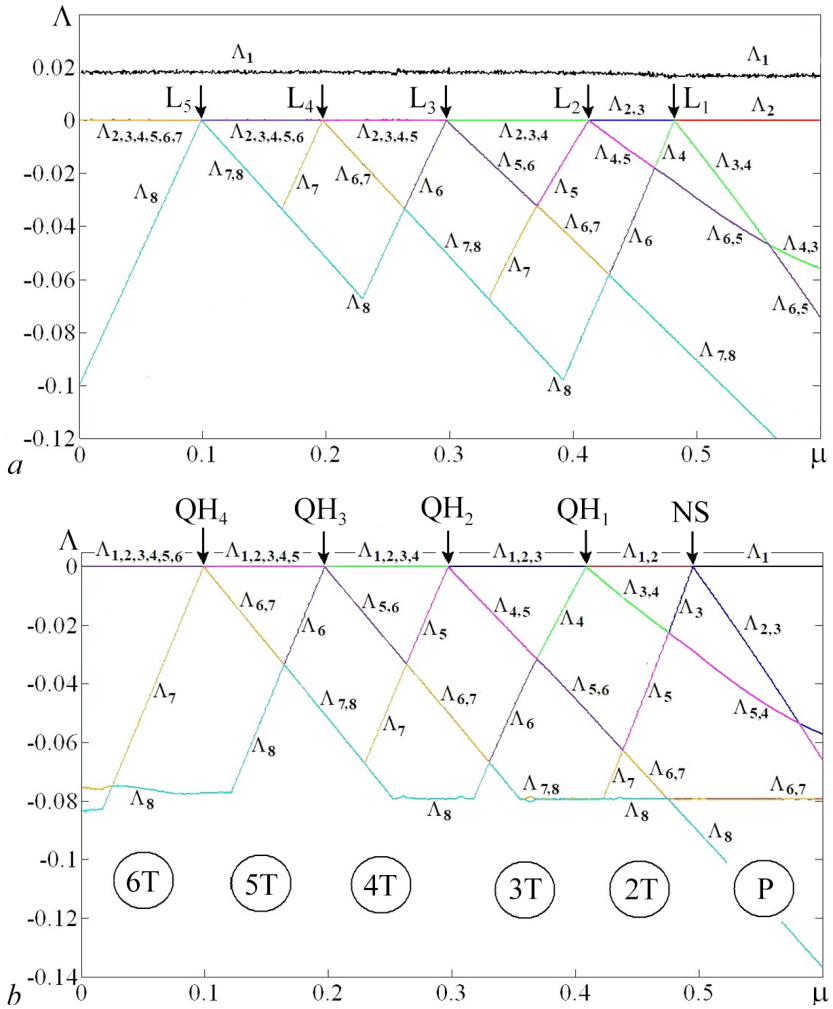

Fig. 4. Graphs of the eight Lyapunov exponents of the model (3) on the van der Pol oscillator's coupling parameter μ for $k = 0.0025$ (a), $k = 0.016$ (b). Parameters of the Kislov–Dmitriev model are $M = 2.75$, $T = 10$, $Q = 20$, $\omega_0 = 0.5$ (color online)

exponents in chaos. In the first case, the behavior of the indicators occurs according to the type of saddle-node bifurcations of the tori (Fig. 3, point Q_2). In the second case, according to the type of quasi-periodic Hopf bifurcations (Fig. 4, a, points L_n).

Now we increase the coupling parameter k of the quasi-periodic and chaotic subsystems to the value $k = 0.016$ (Fig. 4, b). In this case, the chaos is suppressed due to the dissipative nature of communication. The Neumark-Sacker bifurcation NS of the birth of a two-frequency torus with $\Lambda_{1,2} = 0$ from the limit cycle P, for which $\Lambda_1 = 0$, is now observed in the right part of the figure. The threshold of this bifurcation is close to the value of $\mu \approx \lambda_5 = 0.5$, which corresponds to the excitation parameter of the oscillator with the highest value of λ_n. At the same time, for the remaining oscillators $\mu > \lambda_{4,3,2,1}$ and their fluctuations are suppressed.

With decreasing μ, a sequential cascade of quasi-periodic Hopf bifurcations $QH_{1,2,3,4}$ occurs, resulting in the soft birth of a 3-torus, 4-torus, 5-torus, and 6-torus. The criterion for this type of bifurcation is the equality of the corresponding pairs of negative indices (marked in the figure) up to its threshold [46]. This picture can be associated with several steps of the Landau-Hopf scenario. From this we can conclude that the Landau-Hopf scenario observed in an ensemble of van der Pol oscillators is stable and does not collapse when interacting with chaos, if such a relationship is relatively large. Moreover, another Hopf bifurcation is added to produce a stable 6 torus. This is a significant difference

from the Ruel-Takens scenario [17].

Note that the results of Fig. 4 turn out to be similar to the case when the chaotic subsystem is the Ressler system [40]. Thus, their certain versatility is demonstrated. At the same time, in Fig. 3 new developments are being observed. Further, other new features related to a possible change in the configuration of the chaotic attractor for the Kislov-Dmitriev system will be demonstrated.

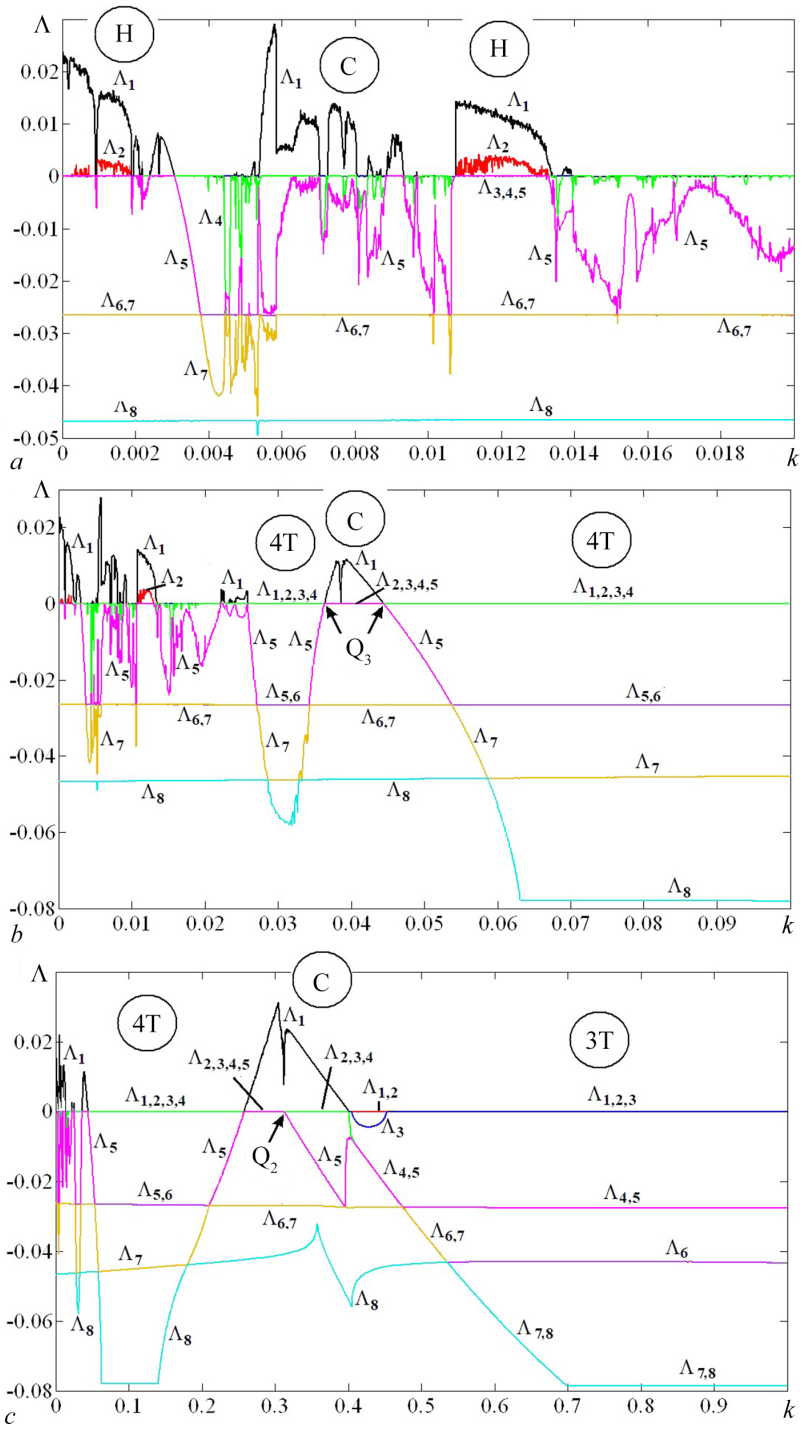

Fig. 5. Graphs of the eight Lyapunov exponents of the model (3) on the coupling parameter k for different ranges of its change; $\mu = 0.25$, $\Delta = 3$. Parameters of the Kislov–Dmitriev model are $M = 3.65$, $T = 10$, $Q = 20$, $\omega_0 = 0.5$ (color online)

5. The case of a modified chaotic attractor

Let us now illustrate the modes that are observed when the main control parameter M of the chaotic subsystem is increased. As we noted, the case $M = 3.65$ corresponds to a change in the configuration of the attractor, Fig. 2, *b*. In Fig. 5 for this case, graphs of eight Lyapunov exponents of the combined system (3) are shown depending on the relationship of subsystems k in different ranges of its variation. The parameters of the quasi-periodic subsystem are chosen similar to Fig. 3, so that in offline mode, a three-frequency mode is observed in this subsystem.

In the area of low coupling in Fig. 5, *a* along with chaos C, a new type of regime is also possible - hyperhaos H with two positive indicators $\Lambda_{1,2} > 0$. The figure clearly shows that in the vicinity of the point $k = 0.012$, the hyperchaotic regime has three zero indices $\Lambda_{3,4,5} = 0$. This is a hyperhaeos with two additional zero indicators. Thus, we extend the Hyperchaos classification started in [53] with additional Lyapunov exponents.

In Fig. 5, *b* the four-frequency mode $4T$ dominates with $\Lambda_{1,2,3,4} = 0$. In the center of the drawing, inside this area, however, there is a window of chaos C with $\Lambda_1 > 0$. This chaos is characterized by four zero exponents $\Lambda_{2,3,4,5} = 0$. Accordingly, at the boundaries of this chaotic window, the fifth exponent Λ_5 turns to zero. Thus, the boundary points of this area are similar to the points of type Q_3 described in Fig. 3.

In the area of high connectivity in Fig. 5, *c* there is a transition from the four-frequency $4T$ to the three-frequency $3T$ mode. This transition also occurs through the chaotic mode window C. Inside this window, on the left there is a mode with four zero indicators $\Lambda_{2,3,4,5} = 0$, and on the right there is a mode with three such indicators $\Lambda_{2,3,4} = 0$. The transition point between these modes is clearly visible. It is similar to the one described in the discussion of Fig. 3 point Q_2.

To summarize the discussion, Fig. 3, 4 and 5, we note that the choice of another chaotic subsystem in relation to the case of the Ressler system [40] led to both the presence of universal patterns and significant features. The latter is especially relevant in the case of a change in the configuration of a chaotic attractor. Therefore, it appears that the marked for Fig. 4 universality occurs when a Feigenbaum type attractor is implemented.

6. The case of chaos with a large value of the senior Lyapunov exponent

Let us now consider the case $M = 8.2$, which, as we noted in section 2, corresponds to a noticeably higher value of the Lyapunov exponent responsible for chaos in the second subsystem. Similar to Fig. 5, *b* (average range of variation of the coupling parameter k) graphs of eight Lyapunov exponents are shown in Fig. 6, *a*. You can see significant changes in the picture.

With a small connection in the left part of Fig. 6, *a* is dominated by hyperchaos H with $\Lambda_{1,2} > 0$ and $\Lambda_{3,4,5} = 0$. Now the hyperchaus areas of H are noticeably wider in terms of bond size than in Fig. 5, *b*.

Further, with the growth of k, there is chaos C with three zero exponents $\Lambda_{2,3,4} = 0$. Areas of weak hyperchausal H are also possible inside it. Note that chaotic and hyperchaotic regions are now observed in a noticeably larger range of values of the coupling parameter. At the same time, the value of the senior indicator Λ_1 is significantly higher. (Compare the ranges along the vertical axis in Fig. 5, *b* and fig. 6, *a*.)

With even greater k coupling, chaos is suppressed, and three-frequency $3T$ and four-frequency $4T$ modes are observed. Let's note an interesting feature. In this case, the birth of a 3-torus occurs when the connection decreases, not increases, as before. This seems somewhat paradoxical, since it seems that the dissipative coupling should suppress fluctuations.

In the figure, the regions $3T$ and $4T$ are separated by the chaos region C with four zero exponents $\Lambda_{2,3,4,5} = 0$. At the same time, no additional bifurcations occur inside it.

An enlarged fragment of graphs in the area of the existence of a three-frequency torus $3T$ is shown in Fig. 6, *b*. It has the appearance of a quasi-periodic window in chaos. When exiting through the left border of this window, successive doubling bifurcations of the three-frequency torus occur $D3T_1$ and $D3T_2$, followed by a transition to chaos with three zero exponents $\Lambda_{2,3,4} = 0$. When passing through the right border of the window, numerous oscillations of the fourth indicator Λ_4 are observed in the vicinity of

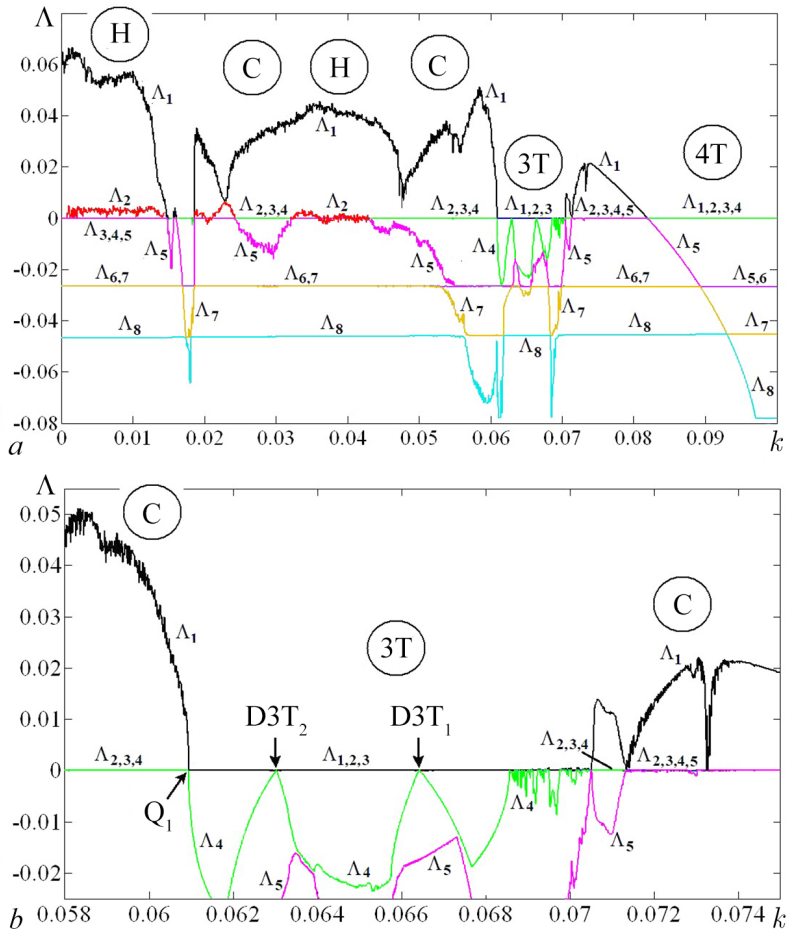

Fig. 6. Зависимость восьми показателей Ляпунова системы (3) от параметра связи k; $\mu = 0.25$, $\Delta = 3$. Общий вид (a) и область квазипериодического окна (b). Параметры системы Кислова–Дмитриева $M = 8.2$, $T = 10$, $Q = 20$, $\omega_0 = 0.5$ (цвет онлайн)

Fig. 6. Graphs of the eight Lyapunov exponents of the model (3) on the coupling parameter k; $\mu = 0.25$, $\Delta = 3$. General view (a) and region of the quasi-periodic window (b). Parameters of the Kislov–Dmitriev generator are $M = 8.2$, $T = 10$, $Q = 20$, $\omega_0 = 0.5$ (color online)

the boundary point. Therefore, the details of the transition to chaos in this case are difficult to describe, we only note the presence of narrow windows of resonant four-frequency tori. With a further increase in the coupling of subsystems k, chaos with three zero indicators $\Lambda_{2,3,4} = 0$ turns into chaos with four such indicators $\Lambda_{2,3,4,5} = 0$. The behavior of the indicators occurs according to the type of saddle-node bifurcation, similar to the point described above Q_2. The only special feature is that the highest exponent Λ_1 has a «dip» at the transition point, dropping to zero.

Conclusion

The interaction of a quasi-periodic subsystem of five non-identical van der Pol oscillators connected in a dissipative manner with a chaotic Kislov-Dmitriev system is considered. The analysis is carried out from the point of view of the possibility of realization and bifurcation of invariant tori of different dimensions, as well as the possibilities of chaos transformation with additional zero Lyapunov exponents.

In the case of three-frequency dynamics in a quasi-periodic subsystem in a combined system, with a decrease in the magnitude of the coupling, a rather complex scenario of transition from three- to four-

frequency dynamics is observed. First, a window of a two-frequency resonant mode is observed, bounded by the lines of saddle-node bifurcations of the tori. Then the three-frequency mode is first restored, but then goes to chaos with three zero Lyapunov exponents. A peculiar bifurcation occurs inside this chaotic region, corresponding to an increase in the number of zero Lyapunov exponents by one. In this case, the behavior of the indicators is partly similar to the saddle-node bifurcation of the tori. Then there is an exit from the chaotic window again, but into the four-frequency region. Further, the scenario is quite universal - the transition to chaos through the doubling of the torus.

When the coupling parameter of the van der Pol oscillators is varied, a cascade of attractor transformations occurs, corresponding to a gradual increase in the number of zero Lyapunov exponents in a chaotic mode. When approaching points of this type, the negative exponents coincide in pairs, which is also typical for quasi-periodic Hopf bifurcations. This pattern is universal in relation to the case of a chaotic Ressler system.

The stability of the Landau-Hopf scenario with respect to interaction with a chaotic subsystem in a certain range of subsystem coupling is shown. It is even possible to increase the dimension of the observed multi-frequency regime and additional Hopf bifurcation with respect to the quasi-periodic subsystem.

With an increase in the nonlinearity parameter in the Kislov-Dmitriev system and a corresponding change in the configuration of the chaotic attractor in the combined system, hyperchaos with three zero Lyapunov exponents may appear.

With an even higher value of this parameter, hyperhaos and chaos with additional zero indicators dominate in a wide range of coupling values. With a decrease in coupling, an inverted order of torus evolution is also observed - the three-frequency turns into a four-frequency one. The device of a quasi-periodic three-frequency window in chaos is also described.

Note that the possibility of new varieties of chaos and hyperchaos may be of interest from the point of view of possible applications, for example, in communication tasks.

References

1. Pikovsky A, Rosenblum M, Kurths J. Synchronization: A Universal Concept in Nonlinear Science. Cambridge: Cambridge University Press; 2001. 411 p. DOI: 10.1017/CBO97805 11755743.
2. Landa PS. Self-Oscillations in Systems with a Finite Number of Degrees of Freedom. M.: LIBROCOM; 2010. 360 p. (in Russian).
3. Balanov AG, Janson NB, Postnov DE, Sosnovtseva OV. Synchronization: From Simple to Complex. Berlin: Springer; 2009. 425 p. DOI: 10.1007/978-3-540-72128-4.
4. Kuznetsov AP, Emelyanova YuP, Sataev IR, Turukina LV. Synchronization in Tasks. Saratov: Nauka; 2010. 256 p. (in Russian).
5. Kuznetsov YuA. Elements of Applied Bifurcation Theory. Cham: Springer; 2023. 703 p. DOI: 10.1007/978-3-031-22007-4.
6. Kuznetsov YuA, Meijer HGE. Numerical Bifurcation Analysis of Maps: From Theory to Software. Cambridge: Cambridge University Press; 2019. 420 p. DOI: 10.1017/9781108585804.
7. Chen X, Qian S, Yu F, Zhang Z, Shen H, Huanga Y, Cai S, Deng Z, Li Y, Du S. Pseudorandom number generator based on three kinds of four-wing memristive hyperchaotic system and its application in image encryption. Complexity. 2020;2020(7):8274685. DOI: 10.1155/2020/8274685.
8. Přibylová L, Ševčík J, Eclerová V, Klimeš P, Brázdil M, Meijer HG. Weak coupling of neurons enables very high-frequency and ultra-fast oscillations through the interplay of synchronized phase shifts. Netw. Neurosci. 2024;8(1):293–318. DOI: 10.1162/netn_a_00351.
9. Bucolo M, Buscarino A, Fortuna L, Gagliano S. Multidimensional discrete chaotic maps. Front. Phys. 2022;10:862376. DOI: 10.3389/fphy.2022.862376.
10. Kopp M. New 7D and memristor-based 8D chaotic systems: Computer modeling and circuit implementation. Journal of Telecommunication, Electronic and Computer Engineering. 2024;16(1): 13–23. DOI: 10.54554/jtec.2024.16.01.003.
11. Kurbako AV, Ponomarenko VI, Prokhorov MD. Adaptive control of nonsynchronous oscillations in network of identical electronic neuron-like generators. Tech. Phys. Lett. 2022;48(10): 38–41. DOI: 10.21883/TPL.2022.10.54796.19328.

12. Korneev IA, Slepnev AV, Semenov VV, Vadivasova TE. Wave processes in a ring of memristively coupled self-excited oscillators. Izvestiya VUZ. Applied Nonlinear Dynamics. 2020;28(3):324–340 (in Russian). DOI: 10.18500/0869-6632-2020-28-3-324-340.
13. Singhal B, Kiss IZ, Li JS. Optimal phase-selective entrainment of heterogeneous oscillator ensembles. SIAM J. Appl. Dyn. Syst. 2023;22(3):2180–2205. DOI: 10.1137/22M1521201.
14. Mircheski P, Zhu J, Nakao H. Phase-amplitude reduction and optimal phase locking of collectively oscillating networks. Chaos. 2023;33(10):103111. DOI: 10.1063/5.0161119.
15. Landau LD. On the problem of turbulence. Dokl. Akad. Nauk USSR. 1944;44(8):339–342 (in Russian).
16. Hopf E. A mathematical example displaying features of turbulence. Comm. Pure Appl. Math. 1948;1:303–322.
17. Ruelle D, Takens F. On the nature of turbulence. Commun. Math. Phys. 1971;20:167–192. DOI: 10.1007/BF01646
18. Anishchenko V, Nikolaev S, Kurths J. Winding number locking on a two-dimensional torus: Synchronization of quasiperiodic motions. Phys. Rev. E. 2006;73(5):056202. DOI: 10.1103/ PhysRevE.73.056202.
19. Anishchenko VS, Nikolaev SM. Transition to chaos from quasiperiodic motions on a four-dimensional torus perturbed by external noise. Int. J. Bifurc. Chaos. 2008;18(9):2733–2741. DOI: 10.1142/S0218127408021956.
20. Anishchenko VS, Nikolaev SM. Stability, synchronization and destruction of quasiperiodic motions. Rus. J. Nonlin. Dyn. 2006;2(3):267–278 (in Russian). DOI: 10.20537/nd0603001.
21. Emelianova YP, Kuznetsov AP, Sataev IR, Turukina LV. Synchronization and multi-frequency oscillations in the low-dimensional chain of the self-oscillators. Physica D. 2013; 244(1):36–49. DOI: 10.1016/j.physd.2012.10.012.
22. Stankevich NV, Kuznetsov AP, Seleznev EP. Chaos and hyperchaos arising from the destruction of multifrequency tori. Chaos, Solitons & Fractals. 2021;147:110998. DOI: 10.1016/j.chaos.2021.110998.
23. Kuznetsov AP, Sataev IR, Sedova YV. Dynamics of three and four non-identical Josephson junctions. Journal of Applied Nonlinear Dynamics. 2018;7(1):105–110. DOI: 10.5890/ JAND.2018.03.009.
24. Kuznetsov AP, Sedova YV, Stankevich NV. Different modes of three coupled generators capable of demonstrating quasiperiodic oscillations. Tech. Phys. Lett. 2022;48(12):56–59. DOI: 10.21883/ TPL.2022.12.54949.19296.
25. Hidaka S, Inaba N, Sekikawa M, Endo T. Bifurcation analysis of four-frequency quasi-periodic oscillations in a three-coupled delayed logistic map. Phys. Lett. A. 2015;379(7):664–668. DOI: 10.1016/j.physleta.2
26. Hidaka S, Inaba N, Kamiyama K, Sekikawa M, Endo T. Bifurcation structure of an invariant three-torus and its computational sensitivity generated in a three-coupled delayed logistic map. IEICE Nonlin. Th. Appl. 2015;6(3):433–442. DOI: 10.1587/nolta.6.433.
27. Kuznetsov AP, Sedova YV, Stankevich NV. Discrete Rössler oscillators: Maps and their ensembles. Int. J. Bifurc. Chaos. 2023;33(15):2330037. DOI: 10.1142/S0218127423300379.
28. Borkowski L, Stefanski A. Stability of the 3-torus solution in a ring of coupled Duffing oscillators. Eur. Phys. J. Spec. Top. 2020;229(12):2249–2259. DOI: 10.1140/epjst/e2020-900276-4.
29. Evstigneev NM. Laminar-turbulent bifurcation scenario in 3D Rayleigh-Benard convection problem. Open Journal of Fluid Dynamics. 2016;6(4):496–539. DOI: 10.4236/ojfd.2016. 64035.
30. Nosov VV, Grigoriev VM, Kovadlo PG, Lukin VP, Nosov EV, Torgaev AV. Astroclimate of specialized stations of the Large solar vacuum telescope: Part II. In: Fourteenth International Symposium on Atmospheric and Ocean Optics/Atmospheric Physics. SPIE; 2008. P. 181-192. DOI: 10.1117/12.783159.
31. Herrero R, Farjas J, Pi F, Orriols G. Nonlinear complexification of periodic orbits in the generalized Landau scenario. Chaos. 2022;32(2):023116. DOI: 10.1063/5.0069878.
32. Krysko AV, Awrejcewicz J, Papkova IV, Krysko VA. Routes to chaos in continuous mechanical systems: Part 2. Modelling transitions from regular to chaotic dynamics. Chaos, Solitons & Fractals. 2012;45(6):709–720. DOI: 10.1016/j.chaos.2012.02.001.
33. Awrejcewicz J, Krysko VA. Scenarios of Transition from Harmonic to Chaotic Motion. In: Chaos in Structural Mechanics. Berlin: Springer; 2008. P. 225–233. DOI: 10.1007/978-3-540-77676-5_10.
34. Kuznetsov AP, Kuznetsov SP, Sataev IR, Turukina LV. About Landau–Hopf scenario in a system of

coupled self-oscillators. Phys. Lett. A. 2013;377(45–48):3291–3295. DOI: 10.1016/ j.physleta.2013.10.013.
35. Kulikov AN. Landau-Hopf scenario of passage to turbulence in some problems of elastic stability theory. Diff. Equat. 2012;48:1258–1271. DOI: 10.1134/S0012266112090066.
36. Kulikov AN, Kulikov DA. A possibility of realizing the Landau—Hopf scenario in the problem of tube oscillations under the action of a fluid flow. Theor. Math. Phys. 2020;203(1): 501–511. DOI: 10.1134/S0040577920040066.
37. Kulikov AN. Bifurcations of invariant tori in second-order quasilinear evolution equations in Hilbert spaces and scenarios of transition to turbulence. J. Math. Sci. 2022;262(6):809–816. DOI: 10.1007/s10958-022-05859-z.
38. Kuznetsov AP, Sedova YV, Stankevich NV. Coupled systems with quasi-periodic and chaotic dynamics. Chaos, Solitons & Fractals. 2023;169:113278. DOI: 10.1016/j.chaos.2023.113278.
39. Kuznetsov AP, Sedova YV. Dynamics of coupled quasiperiodic generator and Rossler system. Tech. Phys. Lett. 2023;49(1):58–61. DOI: 10.21883/TPL.2023.01.55351.19289.
40. Kuznetsov AP, Turukina LV. About the chaos influence on a system with multi-frequency quasi-periodicity and the Landau-Hopf scenario. Physica D. 2024;470B:134425. DOI: 10.1016/j.physd.2024.134425.
41. Dmitriev AS, Kislov VYa. Stochastic Oscillations in Radiophysics and Electronics. M.: Nauka; 1989. 277 p. (in Russian).
42. Dmitriev AS. Forty years of the Dmitriev-Kislov ring oscillator model. Izvestiya VUZ. Applied Nonlinear Dynamics. 2024;32(4):423–427 (in Russian). DOI: 10.18500/0869-6632-003119.
43. Kuznetsov SP. Dynamic Chaos. M.: Fizmatlit; 2001. 295 p. (in Russian).
44. Dmitriev A, Efremova E, Maksimov N, Panas A. Chaos Generation. M.: Tekhnosfera; 2012. 424 p. (in Russian).
45. Emelyanova YP, Kuznetsov AP. Synchronization of coupled van der pole and Kislov-Dmitriev self-oscillators. Tech. Phys. 2011;56(4):435–442. DOI: 10.1134/S106378421104013X.
46. Vitolo R, Broer H, Simó C. Quasi-periodic bifurcations of invariant circles in low-dimensional dissipative dynamical systems. Regul. Chaot. Dyn. 2011;16:154–184. DOI: 10.1134/S1560354 711010060.
47. Broer H, Vitolo R, Simó C. Quasi-periodic Hénon-like attractors in the Lorenz-84 climate model with seasonal forcing. In: EQUADIFF 2003. 22–26 July 2003, Hasselt, Belgium. 2005. P. 601–607. DOI: 10.1142/9789812702067_0100.
48. Broer H, Simó C, Vitolo R. Bifurcations and strange attractors in the Lorenz-84 climate model with seasonal forcing. Nonlinearity. 2002;15(4):1205–1267. DOI: 10.1088/0951-7715/15/4/312.
49. Broer HW, Simó C, Vitolo R. Chaos and quasi-periodicity in diffeomorphisms of the solid torus. Discrete Contin. Dyn. Syst. Ser. B. 2010;14(3):871–905. DOI: 10.3934/dcdsb.2010.14.871.
50. Popova ES, Stankevich NV, Kuznetsov AP. Cascade of invariant curve doubling bifurcations and quasi-periodic Hénon attractor in the discrete Lorenz-84 model. Izvestiya of Saratov University. Physics. 2020;20(3):222–232 (in Russian). DOI: 10.18500/1817-3020-2020-20-3-222-232.
51. Stankevich NV, Shchegoleva NA, Sataev IR, Kuznetsov AP. Three-dimensional torus breakdown and chaos with two zero Lyapunov exponents in coupled radio-physical generators. J. Comput. Nonlinear Dynam. 2020;15(11):111001. DOI: 10.1115/1.4048025.
52. Grines EA, Kazakov A, Sataev IR. On the origin of chaotic attractors with two zero Lyapunov exponents in a system of five biharmonically coupled phase oscillators. Chaos. 2022;32(9):093105. DOI: 10.1063/5.0098163.
53. Garashchuk I, Kazakov A, Sinelshchikov D. Scenarios for the appearance of strange attractors in a model of three interacting microbubble contrast agents. Chaos, Solitons & Fractals. 2024;182: 114785. DOI: 10.1016/j.chaos.2024.114785.
54. Karatetskaia E, Shykhmamedov A, Kazakov A. Shilnikov attractors in three-dimensional orientation-reversing maps. Chaos. 2021;31(1):011102. DOI: 10.1063/5.0036405.
55. Shykhmamedov A, Karatetskaia E, Kazakov A, Stankevich N. Scenarios for the creation of hyperchaotic attractors in 3D maps. Nonlinearity. 2023;36(7):3501–3541. DOI: 10.1088/1361-6544/acd044.
56. Muni SS. Ergodic and resonant torus doubling bifurcation in a three-dimensional quadratic map.

Nonlinear Dyn. 2024;112(6):4651–4661. DOI: 10.1007/s11071-024-09284-6.
57. Muni SS. Persistence of resonant torus doubling bifurcation under polynomial perturbations. Franklin Open. 2025;10:100207. DOI: 10.1016/j.fraope.2024.100207.